coatings

Article

Research on a Multi-Objective Optimization Design for the Durability of High-Performance Fiber-Reinforced Concrete Based on a Hybrid Algorithm

Xingyu Wang [1], Fengkun Cui [1,*], Long Cui [2] and Di Jiang [3]

[1] School of Civil Engineering, Shandong Jiaotong University, 5 Jiaoxiao Road, Jinan 250357, China; 21107030@stu.sdjtu.edu.cn
[2] Shandong Provincial Academy of Building Research Co., Ltd., 29 Wuyingshan Road, Jinan 250031, China; 15550025256@163.com
[3] Shandong Huiyou Municipal Landscape Group Co., Ltd., 29 East Automobile Factory Road, Jinan 250031, China
* Correspondence: 204118@sdjtu.edu.cn

Abstract: To achieve durable high-performance fiber-reinforced concrete that meets economic requirements, this paper introduces a hybrid intelligent framework based on the Latin hypercube experimental design, response surface methodology (RSM), and the NSGA-III algorithm for optimizing the mix design of high-performance fiber-reinforced concrete. The developed framework allows for the prediction of concrete performance and obtains a series of Pareto optimal solutions through multi-objective optimization, ultimately identifying the best mix proportion. The decision variables in this optimization are the proportions of various materials in the concrete mix, with concrete's frost resistance, chloride ion permeability resistance, and cost as the objectives. The feasibility of this framework was subsequently validated. The results indicate the following: (1) The RSM model exhibits a high level of predictive accuracy, with coefficient of determination (R-squared) values of 0.9657 for concrete frost resistance and 0.9803 for chloride ion permeability resistance. The RSM model can be employed to construct the fitness function for the optimization algorithm, enhancing the efficiency of multi-objective optimization. (2) The NSGA-III algorithm effectively balances durability and cost considerations to determine the optimal mix proportion for the concrete. After multi-objective optimization, the chloride ion permeability resistance and frost resistance of the high-performance fiber-reinforced concrete improved by 38.1% and 6.45%, respectively, compared to the experimental averages, while the cost decreased by 2.53%. The multi-objective optimization method proposed in this paper can be applied to mix design for practical engineering projects, improving the efficiency of concrete mix design.

Keywords: high-performance fiber-reinforced concrete; durability; multi-objective optimization; Latin hypercube experimental design; response surface methodology; NSGA-III

check for updates

Citation: Wang, X.; Cui, F.; Cui, L.; Jiang, D. Research on a Multi-Objective Optimization Design for the Durability of High-Performance Fiber-Reinforced Concrete Based on a Hybrid Algorithm. *Coatings* **2023**, *13*, 2054. https://doi.org/10.3390/coatings13122054

Academic Editors: Ionut Ovidiu Toma and Ofelia-Cornelia Corbu

Received: 31 October 2023
Revised: 1 December 2023
Accepted: 4 December 2023
Published: 7 December 2023

1. Introduction

High-performance fiber-reinforced concrete (HPFRC) exhibits superior ductility and toughness compared to ordinary concrete [1–4]. As a result, HPFRC has found extensive applications in practical engineering in recent years [5–7]. Concrete structures in the northern coastal regions of China are not only subject to the detrimental effects of chloride salt intrusion but also the unique freeze−thaw cycles in the northern sea areas. The nonlinear coupled effects arising from the interaction of these two factors accelerate material degradation and performance deterioration of concrete components, highlighting the prominent issue of durability [8–11]. Besides adopting measures from a structural design perspective, such as implementing protective coatings and increasing the thickness of the concrete protective layer, it is imperative to conduct research on enhancing the concrete's inherent durability.

The durability of concrete mainly considers frost resistance and chloride ion permeability, as these two factors directly affect the long-term performance and safety of concrete structures. The frost resistance of concrete refers to its performance under low temperatures and freeze−thaw cycling conditions. The volume expansion of water in concrete during freezing may lead to the generation and expansion of microcracks, thereby reducing the structural integrity and load-bearing capacity of the concrete. In cold winter regions, frost resistance is a key factor in ensuring the integrity and safety of concrete structures; the impermeability of chloride ions involves the permeability resistance of concrete to chloride ions. The penetration of chloride ions (mainly from salt water or seawater) is one of the main reasons for the corrosion of steel bars in concrete. Corrosion of steel bars can seriously affect the integrity and durability of concrete structures. Therefore, improving the impermeability of concrete to chloride ions can effectively prevent steel corrosion and prolong the service life of concrete structures. By improving these two properties, the durability and service life of concrete structures can be significantly improved [12–16]. Numerous scholars have studied the parameters that affect the durability of concrete, and the research results indicate that the frost resistance and chloride ion permeability of concrete are mainly influenced by the mix ratio of raw materials such as cement, water, aggregates, and additives [17–21]. These factors determine the durability and service life of concrete structures. Currently, most people refer to the "General Concrete Mix Design Code" [22] for mix proportion design and employ orthogonal experiments to seek the optimal mix. However, when using orthogonal experiments to find the best mix, there are drawbacks, such as a substantial workload, low predictive accuracy, and suboptimal results [23–25]. Additionally, it cannot establish a clear functional relationship between factors and response values in a specified region [26,27].

To unravel the complex relationship between concrete mix proportions and resistance to freezing and chloride ion penetration, statistical models are often introduced in relevant experiments and analyses. The response surface method (RSM) is commonly used to predict the durability of concrete [28,29]. RSM is a product of the fusion of mathematics and statistics, capable of establishing mathematical models between multiple factors and one or more response values with minimal experimental data [30,31]. It evaluates the impact of interaction among factors on response values, determines the optimal response values, and offers advantages over orthogonal experiments, such as requiring fewer trials, lower costs, and higher predictive accuracy [32]. Naraindas Bheel et al. [33] employed RSM's central composite design (CCD) to establish a relationship between 13 different raw material contents and eight target values in engineered cementitious composites (ECC). They validated the predicted values through experiments, and the results showed a strong correlation between the predicted values and the experimental data. Wang et al. [34] used RSM's central composite design to perform experimental design on basalt fiber foam concrete and achieved multi-objective optimization by incorporating utility functions. Zhang et al. [35] utilized RSM with a Box−Behnken design (BBD) to obtain the optimal aggregate grading and admixture dosage for permeable concrete made with recycled aggregates. The aforementioned studies demonstrate that the application of RSM in optimizing construction material mixtures offers significant advantages. However, research on the application of RSM for optimizing the mix proportions of high-performance fiber-reinforced concrete is relatively scarce.

In addition, when designing the mix proportion of concrete, the economic cost requirements of the engineering application must be taken into consideration [36]. However, there exists a conflict between the durability of concrete and the economic cost [37]. In recent years, the nondominated sorting genetic algorithm (NSGA) has been applied to concrete mix proportion design, providing a new solution for multi-objective optimization problems (MaOPs) [38,39]. The basic NSGA proposed by Srinivas and Deb [40] has been widely used to solve MaOPs, but it comes with high computational complexity. Therefore, Deb et al. [41]

proposed the NSGA-II algorithm, which incorporates elite preservation, fast nondominated sorting, and crowding distance selection operators. NSGA-II has advantages such as fast operation speed and good convergence. However, the crowding distance selection in three-dimensional and higher dimensional objective spaces may not be effective, leading to a reduction in the diversity of solutions. Reducing the complexity of the dataset may potentially improve the accuracy of deep learning models. Simplifying the process of the dataset can help deep learning models learn key features related to problems more effectively, thereby improving their performance and generalization ability. In practice, finding the appropriate level of dataset complexity often requires adjustments based on domain knowledge and experimental results [42,43].

Hence, Deb and Jain [44] introduced NSGA-III. In comparison, NSGA-III directly searches for the Pareto optimal solutions in the space, eliminating issues such as transformation parameters and information loss, making the search process simple and intuitive. Furthermore, the inherent characteristics of genetic algorithms make NSGA-III widely adaptable; the combination of continuous and discrete variable inputs does not significantly affect the algorithm's performance. NSGA-III guides the selection of nondominated solutions using uniformly distributed reference points in space, effectively ensuring the widespread distribution and diversity of nondominated solutions in high-dimensional objective spaces. In fact, NSGA-III is currently recognized as the best algorithm for MaOPs [45–47]. At present, NSGA-III has been applied and demonstrated effective in multi-objective optimization in various fields such as automation technology, water supply, and aerospace [48–50]. However, there is a notable scarcity of reported applications of NSGA-III in the domain of concrete mix proportion design.

This study commences with the utilization of a Latin hypercube experimental design methodology for mix proportion development. Subsequently, upon obtaining specimen samples, concrete specimens are fabricated, and frost resistance, as well as chloride ion permeability tests, are conducted. This facilitates the acquisition of the relative dynamic modulus of elasticity and chloride ion migration coefficient for concrete specimens corresponding to various mix proportions. A response surface model is then established. Subsequently, the constructed response surface model is integrated with the NSGA-III algorithm, thereby achieving multi-objective optimization for high-performance fiber-reinforced concrete.

2. Preliminary Information

2.1. Latin Hypercube Design

Before designing and optimizing the mix proportion of high fiber reinforced concrete, it is necessary first to use certain experimental design methods to sample the design space and generate a certain number of sample points. The commonly used experimental design methods include orthogonal design, uniform design, Latin hypercube sampling, etc. The Latin hypercube design (LHD) is a method used for experimental design and sampling design space, and its core idea is to ensure that each level value is evenly and randomly paired with other levels in each dimension. This design approach helps to achieve wide coverage in the design space while reducing the number of samples, which improves sampling efficiency compared to completely random sampling methods.

The key elements to ensure that the results of Latin hypercube sampling are unbiased and effective are as follows:

(1) Uniformity: The core goal of LHD is to ensure a uniform distribution of sample points in each dimension, ensuring comprehensive coverage of the design space.
(2) Randomness: By randomly selecting sample points on each dimension, LHD ensures that sufficient randomness is introduced during the sampling process so that the results are not affected by specific points.
(3) Reduce sample size: Compared to comprehensive sampling, LHD reduces the required sample size by effectively selecting sample points, improving sampling efficiency.

When applying LHD to design space sampling: In a multidimensional design space, LHD divides each dimension into equal intervals and selects a sample point within each interval to ensure a uniform selection of sample points throughout the entire design space. This helps to capture representative features of the design space rather than just sampling in certain local areas. The basic theory is as follows:

Assuming the probability distribution function of each element of the K-dimensional random variable x is F_i (I = 1, 2, . . . , K). The elements of vector x are independent of each other, and each element is sampled N times, which is the value of the jth (j = 1, 2, . . . , N) sampling of the k (k = 1, 2, . . . , K) th element. Define $N \times$ K-dimensional matrix P. Each column of P is composed of a random arrangement of elements in the sequence {1, 2, . . . , N}. If the random variable ξ_{jk} follows a uniform distribution on the interval [0,1], the result obtained after sampling is:

$$xjk = F_k^{-1}[(pjk - 1 + \xi jk)/N] \tag{1}$$

In the equation, p_{jk} is $N \times$ The j row and k column elements of the K-dimensional matrix P.

Assuming the existence of function h(x), the unbiased estimate of the mean E(h(x)) of function h(x) is defined as:

$$\overset{\frown}{h} = \sum_{j=1}^{N} \mathrm{h}(x_j)/N \tag{2}$$

The variance of the unbiased estimate $\overset{\frown}{h}$ for simple random sampling is:

$$D(\overset{\frown}{h}) = D(h(x))/N \tag{3}$$

The variance of the unbiased estimation of Latin hypercube is:

$$D(\overset{\frown}{h}) = D(h(x))/N + (N-1)cov(h(x_{1n}), h(x_{2n}))/N \tag{4}$$

It can be proven that the probability of $(N-1)cov(h(x_{1n}), h(x_{2n}))/N$ approaches a negative value. Therefore, Latin hypercube sampling is easier to converge than random sampling.

The key factor in ensuring unbiased and efficient results when dividing the experimental domain of LHD lies in its design method, which ensures the representativeness of the samples by uniformly and randomly selecting sample points. This helps to explore the design space more effectively in tasks such as experimental design and parameter optimization, reducing the number of required experiments and improving the efficiency and cost-effectiveness of experiments. Numerous scholars have further verified the above viewpoint through theoretical research [51,52]. Therefore, we select LHD to determine the sample points required for concrete mix design.

2.2. Response Surface Model

Response surface methodology is a method of optimizing experimental conditions suitable for fitting the complex nonlinear response relationship between optimization objectives and experimental factors. The multivariate second-order response surface model is generally represented by the following equation.

$$y(x) = \beta_0 + \sum_{i=1}^{m} \beta_i x_i + \sum_{i=1}^{m} \beta_{ii} x_i^2 + \sum_{i<j}^{m} \beta_{ij} x_i x_j \tag{5}$$

In the equation, $y(x)$ represents the response objective function; x_i, x_j represents the i-th and jth experimental factors; β_0 represents a constant term, β_i, β_{ii}, β_{ij} represents various coefficients; m represents the number of parameters to be optimized.

2.3. NSGA-III Algorithm

Nondominated sorting genetic algorithm III (NSGA-III) is a widely used multi-objective optimization (MO) algorithm designed to solve two types of problems: maintaining good solution diversity and optimizing solution convergence. This is an improved version that compensates for the shortcomings of its predecessor, NSGA-II, in losing solution diversity and accuracy when dealing with high-dimensional problems.

The core operations of NSGA-III include nondominated sorting, calculation of crowding distance, evolutionary operations (selection, crossover, and mutation), and environmental selection. Its unique features and mechanisms are mainly reflected in the following points:

Reference point mechanism: NSGA-III introduces the concept of reference points to improve the diversity of solutions. During the initialization phase, the algorithm generates a set of reference points. These reference points are used in each generation to select solutions and create the next generation. The solutions are selected to minimize their distance from the reference point. This ensures the distribution and coverage of the understanding.

Multiple nondominated levels: NSGA-III implements multiple nondominated sorting of solutions. The solution is divided into several nondominated layers, each layer being superior to its lower layer. In each generation, the algorithm prioritizes solutions from higher levels.

Crowding distance: In order to maintain population diversity, NSGA-III uses a crowding distance mechanism. Among solutions with the same level, solutions with lower crowding (i.e., solutions with more "space" around them) will be preferred. This helps to prevent the algorithm from overly focusing on a small portion of the search space, thereby achieving diversity of understanding.

Additional parents: When selecting solutions to create the next generation, NSGA-III not only considers the current parents (so-called P population) but also considers new possible solutions generated through offspring (so-called Q population). This is also known as a "joint population", and this design can increase the diversity of solutions and accelerate the speed of evolution.

Special environment selection strategy: When a new P population needs to be selected, NSGA-III will first select nondominated solutions and add excess solutions to the population according to the reference point allocation strategy, which ensures the convergence of the solution in multi-objective optimization problems.

Overall, NSGA-III effectively addresses multi-objective optimization problems through these mechanisms, overcomes weaknesses in the diversity of solutions, and provides uniformly distributed solutions at the Pareto frontier, thereby enhancing the convergence of the algorithm. This characteristic makes NSGA-III perform well in handling practical engineering problems such as high-performance fiber-reinforced concrete. Meanwhile, to balance the relationships between objective functions, an adaptive normalization technique is introduced. The ideal point for the population, $S_t = F_1 \cup F_2 \cup \ldots \cup F_l$, is defined as the minimum point attained by the population St on each respective objective. When normalizing multiple objectives, it is necessary to construct hyperplanes by seeking limit points to determine intercepts. Subsequently, the obtained intercepts are utilized to normalize the objectives individually. Considering that the mixed NSGA-III produces a Pareto solution set that closely approximates the actual optimal solution set of the problem, the obtained Pareto solution set after multi-objective optimization can be considered the final optimal solution. Therefore, the corresponding maximum value of the *i*-th objective in the corresponding population can be used to replace the intercept of the corresponding objective.

$$f_i^n(x) = \frac{f_i(x) - z_i^{\min}}{z_i^{\max} - z_i^{\min}}, \text{for } i = 1, 2, \cdots, M \tag{6}$$

In the formula, M represents the number of targets; x represents the decision variable; $f_i(x)$ represents the target value of x on the corresponding i-th target; $z_i^{\min}$ and $z_i^{\max}$ represent the minimum and maximum values of the population on the *i*-th target, respectively; $f_i^n(x)$ represents the normalized target value of the *i*-th target.

3. Method

This paper presents a smart hybrid system designed for simultaneously optimizing both the durability and cost-effectiveness of high-performance fiber-reinforced concrete, achieving multi-objective enhancement. Figure 1 shows the flowchart of the model. The overall framework of this article is divided as follows.

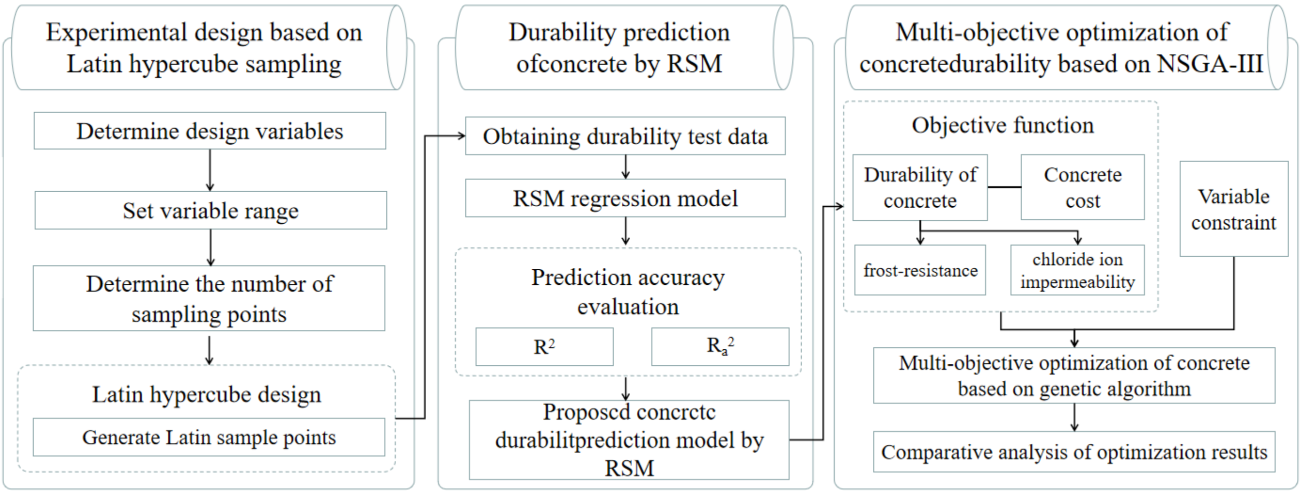

Figure 1. Flow chart of the proposed model.

3.1. Latin Hypercube Experimental Design

(1) Determine design variables

Determine the key design variables that affect the mix design of high-performance fiber-reinforced concrete, such as water content, cement content, fly ash content, fine aggregate content, coarse aggregate content, water-reducing agent content, and fiber content. The design variables determined in this article are all independent variables, further ensuring that the Latin hypercube sampling results are unbiased.

(2) Set variable range

To ensure the rationality of the mix proportion of high-performance fiber-reinforced concrete, a suitable range of raw material content is set through consulting relevant literature and preliminary mix proportion tests [53–55].

(3) Determine the number of sampling points

Determine the number of Latin hypercube sampling points to generate. This depends on the complexity of the problem and the sampling requirements for the design space.

(4) Generate Latin hypercube sampling

Generate uniformly distributed sampling points within the design variable range using the Latin hypercube sampling method. This article uses the pyDOE library in Python for Latin hypercube sampling.

(5) Durability test and data preprocessing

Using the generated Latin hypercube sampling points as input parameters for concrete mix proportions, prepare concrete and conduct corresponding frost resistance and chloride ion permeability tests to obtain the relative dynamic elastic modulus and chloride ion migration coefficient corresponding to different sample points. The dimensions and attribute ranges of various input variables representing the proportion of raw materials in concrete are not the same and cannot be directly compared. Therefore, formula (7) is used to unify input variables and output energy consumption into intervals [−1,1] to achieve data normalization and unify the dimensions of variables so that each feature plays a role in the prediction process.

$$y = (y_{\max} - y_{\min}) \times \frac{x - x_{\min}}{x_{\max} - x_{\min}} + y_{\min} \tag{7}$$

3.2. Establishing an RSM Model

Based on the durability test results, a response surface model is constructed to obtain the nonlinear relationship between the durability of high-performance fiber-reinforced concrete and the amount of raw materials added. The reliability of the RSM model is evaluated using correlation coefficient R^2 and adjustment coefficient ${R_a}^2$. Generally, $R^2 \in [0,1]$, and the closer R^2 is to 1, the higher the fitting accuracy of the response surface model, usually requiring $R^2 > 0.9$. The calculation formula is shown in the following equation.

$$R^2 = 1 - \frac{S_r}{S_m + S_r} \tag{8}$$

$$R_a^2 = \frac{S_r / D_r}{(S_m + S_r)/(D_m + D_r)} \tag{9}$$

In the formula, S_r is the sum of squares of the residuals; S_m is the sum of regression squares; D_r is the residual degree of freedom; D_m is the degree of freedom of regression.

3.3. Multi-Objective Optimization Based on NSGA-III

3.3.1. Concrete Durability Objective Function

Based on the response surface model, construct a chloride ion impermeability model for high-performance fiber-reinforced concrete, represented by f_1 and the frost resistance model, represented by f_2.

$$f_1 = \max[RSM(x_1, x_2, \ldots, x_n)] \tag{10}$$

$$f_2 = \min\left[RSM\left(x_1', x_2', \ldots, x_n'\right)\right] \tag{11}$$

Among them, x_1, x_2, …, x_n are the input variables of the response surface model used for prediction.

3.3.2. Economic Cost Function

In practical engineering, concrete structure needs to control the economic cost of concrete while meeting the durability requirements. The objective function f_3 of optimizing the economic cost of concrete is expressed as:

In practical engineering applications, it is necessary to balance the cost and durability of high-performance fiber-reinforced concrete. The function f_3 with cost as the optimization objective is represented as follows:

$$f_3 = \min\sum_{i=1}^{n} v_i x_i \tag{12}$$

Among them, x_i represents the i-th raw material that constitutes high-performance fiber-reinforced concrete, and v_i represents the cost of the i-th raw material.

3.3.3. Constraint Condition Setting

To guarantee an effective and practical composition of high-performance fiber-reinforced concrete, establishing an appropriate range for the content of raw materials and setting suitable constraints is essential. The general form of constraints is:

$$b_{\min} \leq x_i \leq b_{\max} \tag{13}$$

In the formula, x_i represents the raw material of the i-th high-performance fiber-reinforced concrete, while $b_{\min}$ and $b_{\max}$ represent the minimum amount of the i-th raw material, respectively.

3.3.4. Multi-Objective Optimization Based on NSGA-III

Using the MATLAB platform, implement the NSGA-III algorithm with the aim of enhancing the durability of concrete while concurrently minimizing its cost. The result of this algorithm will be the set of Pareto optimal solutions for concrete mix proportions. The fundamental steps for acquiring the Pareto optimal solution set through the NSGA-III algorithm include:

(1) Initialize population: Randomly generate an initial population, where each individual contains the variables of the problem and the values of the objective function.
(2) Set algorithm parameters: Determine the parameters of the algorithm, such as population size, crossover probability, mutation probability, maximum number of iterations, etc.
(3) Execute the NSGA-III algorithm: Use the core steps of the NSGA-III algorithm, including nondominated sorting, crowding allocation, genetic operations (crossover and mutation), etc. These steps will gradually optimize the individuals in the population, generating a set of approximate Pareto frontier solutions.
(4) Termination condition: Define the stopping condition, such as reaching the maximum number of iterations, Pareto frontier convergence, etc.
(5) Obtaining results: After the algorithm runs, the final Pareto frontier solution set is obtained, which represents the nondominated solution set of the problem.
(6) Analysis results: For each Pareto frontier solution, analyze its performance on various objective functions and select the solution that best meets the requirements of the problem.

4. Case Analysis

4.1. Engineering Background

The Xinan River Grand Bridge is situated on Binhai East Road, Laishan District, Yantai City, Shandong Province, China. It was completed in 2003 and serves as a major transportation artery connecting the Laishan and Muping districts. Given its substantial traffic volume, the project environment is depicted in Figure 2. This sea-crossing bridge is located in the frozen waters of northern China. Concrete components within the fluctuating water levels are subjected not only to chloride erosion but also to the unique freeze−thaw cycles prevalent in northern maritime regions. The coupling effect arising from the interaction of these two factors accelerates the material degradation and performance deterioration of the concrete elements. Consequently, the durability issues of the bridge are notably prominent.

To address these challenges, this study focuses on the development of high-performance fiber-reinforced concrete to enhance the structural durability of the Xinan River Grand Bridge.

According to the "Durability Design Standard for Concrete Structures" [56], the specimens are placed in a rapid freeze−thaw machine for 300 freeze−thaw cycles, and the relative dynamic elastic modulus of the specimens is measured to represent the frost resistance of the concrete. The chloride ion migration coefficient of the concrete after 28 days of curing is measured using the RCM method to represent the chloride ion permeability of the concrete. This study focuses on the C50 concrete used in the aforementioned projects. Figure 3a,b shows photos of the relative dynamic elastic modulus test and chloride ion migration coefficient of the tested concrete specimens. The raw materials used in this experiment include cement produced by Shandong Shanshui Group (Jinan, China), first-class fly ash produced by Hengyuan New Materials Co., Ltd., (Dongying, China), polycarboxylic acid high-efficiency water-reducing agent produced by Kaili Chemical, and polyacrylonitrile fiber produced by Huixiang Fiber, among others.

Figure 2. Photograph of the project.

(**a**) (**b**)

Figure 3. Concrete durability tests. (**a**) Frost resistance test; (**b**) RCM test.

4.2. Proportion Design of High-Performance Fiber-Reinforced Concrete Based on LHD

This study mainly considers the influence of seven factors on the two durability indicators of high-performance fiber-reinforced concrete. These seven factors are water content (x_1), cement content (x_2), fly ash content (x_3), fine aggregate content (x_4), coarse aggregate content (x_5), water reducer content (x_6), and fiber content (x_7). This article uses the pyDOE library in Python to conduct Latin hypercube sampling and obtain 36 sets of Latin experimental samples. The design variables determined in this article are all independent variables, further ensuring that the Latin hypercube sampling results are unbiased.

The response surface model contains $1 + 2m + m\ (m - 1)/2$ coefficients to be solved. When m = 7, the test should include at least 36 sets of test sample points, and the test arrangement in Table 1 meets the requirements.

Table 1. Initial Data Information.

Item	Units	Parameter Type	Date (36)		
			Min	Max	Ave
x_1	kg/m^3	Input	135	165	150
x_2	kg/m^3	Input	385	435	410
x_3	kg/m^3	Input	33	126	79.5
x_4	kg/m^3	Input	680	700	690
x_5	kg/m^3	Input	1116	1142	1129
x_6	kg/m^3	Input	4.16	5.77	4.965
x_7	kg/m^3	Input	24.36	73.08	48.72

4.3. Prediction of Durability Utilizing a Response Surface Model

4.3.1. Collection of Sample Data

Using the Latin hypercube experimental design, 36 sets of Latin test samples were obtained and subjected to rapid freeze−thaw test and RCM test, respectively. The results of freeze−thaw resistance and chloride ion permeability of 36 sets of Latin test samples were obtained, as shown in Table 2.

Table 2. Sample Dataset and Related Information.

Item	Units	Parameter Type	Date (36)				
			Min	Max	Ave	Median	SD
x_1	kg/m^3	Input	135	165	150	150.00	9.64
x_2	kg/m^3	Input	385	435	410	410.00	16.08
x_3	kg/m^3	Input	33	126	79.5	79.50	29.91
x_4	kg/m^3	Input	680	700	690	690.00	6.43
x_5	kg/m^3	Input	1116	1142	1129	1129.00	8.36
x_6	kg/m^3	Input	4.16	5.77	4.965	4.96	0.51
x_7	kg/m^3	Input	24.36	73.08	48.72	48.72	15.66
RD	%	Output	85.1	91.2	88.15	87.78	1.62
CP	10^{-12} m^2/s	Output	1.6	3.5	2.55	2.58	0.53
CO	yuan	Output	638.54	1068.39	853.46	853.47	123.38

4.3.2. Evaluation of Forecast Results

(1) Frost resistance model of concrete based on response surface.

According to the results of 36 groups of data, a concrete frost resistance model based on response surface is constructed, and a multiple regression model with water content, cement content, fly ash content, fine aggregate content, coarse aggregate content, water reducer content, and fiber content as response values is obtained. See Figure 4 and Table 3 for verification results.

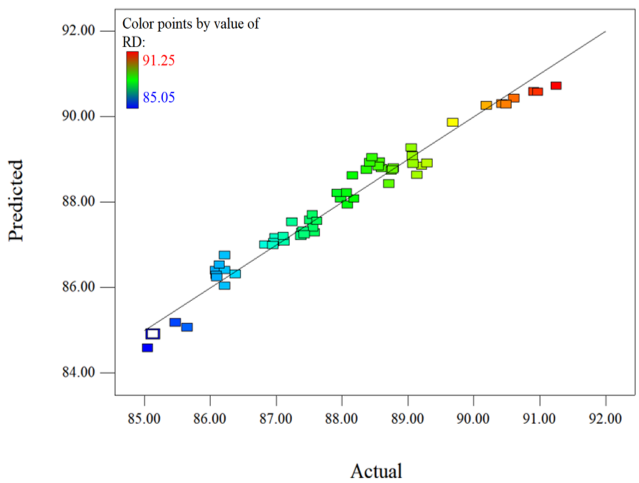

Figure 4. Accuracy verification of approximate model for frost resistance response surface.

Table 3. Error Analysis of Frost Resistance Regression Model.

Items	Std. Dev.	C.V.%	R^2	$R_a{}^2$
value	0.45	0.51	0.9657	0.9111

As can be seen from Figure 4 and Table 3, the determination coefficient R^2 of the regression model is 0.9657, which is close to 1, indicating that the predicted relative dynamic elastic modulus of high-performance fiber-reinforced concrete is highly correlated with the actual value. The adjustment coefficient $R_a{}^2$ is 0.9111, which is greater than 0.8; the coefficient of variation is 0.51%, less than 10%. It shows that the second-order response surface model has a good fitting degree and can effectively and accurately predict the relative dynamic elastic modulus of high-performance fiber-reinforced concrete under different mix proportions.

(2) Response surface-based model for chloride ion permeability resistance

Based on 36 sets of data results, a response surface-based chloride ion permeability resistance model was constructed to obtain a multiple regression model with response values of water content, cement content, fly ash content, fine aggregate content, coarse aggregate content, water-reducing agent content, and fiber content. The validation results are shown in Figure 5 and Table 4.

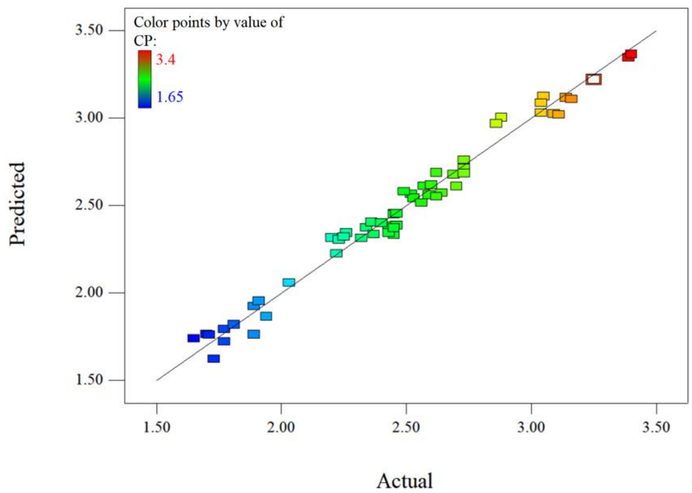

Figure 5. Accuracy verification of chloride ion impermeability response surface approximation model.

Table 4. Error analysis of regression model for chloride ion impermeability.

Items	Std. Dev.	C.V.%	R^2	$R_a{}^2$
value	0.10	4.08	0.9803	0.9490

From Figure 5 and Table 4, it can be seen that the determination coefficient R^2 of the regression model is 0.9803, which is close to 1, indicating that the predicted value of the chloride ion migration coefficient of high-performance fiber-reinforced concrete is highly correlated with the actual value. The adjustment coefficient $R_a{}^2$ is 0.9490, greater than 0.8; the coefficient of variation is 4.08%, less than 10%. This indicates that the second-order response surface model has a good fitting degree and can effectively and accurately predict the chloride ion migration coefficient of high-performance fiber-reinforced concrete under different mix ratios.

4.4. Multi-Objective Optimization Utilizing NSGA-III

4.4.1. Formulation of the Objective Function

In engineering endeavors, enhancing the durability of concrete typically accompanies increased costs. To strike a balance between cost-effectiveness and ensuring optimal durability, a multi-objective optimization approach is employed.

(1) Optimization objective function of concrete frost resistance based on response surface model.

The response surface model serves the purpose of predicting the relative dynamic elastic modulus of concrete. Subsequently, the objective function for optimizing the frost resistance of concrete is formulated as follows:

$$\max \cdot f_1 = \max[RSM(x_1, x_2, \ldots, x_7)] = \beta_0 + \sum_{i=1}^{7} \beta_i x_i + \sum_{i=1}^{7} \beta_{ii} x_i^2 + \sum_{i<j}^{7} \beta_{ij} x_i x_j \tag{14}$$

In the formula, x_1, x_2, x_3, x_4, x_5, x_6, and x_7 respectively represent the water content, cement content, fly ash content, fine aggregate content, coarse aggregate content, water-reducing agent content, and fiber content.

(2) Optimization objective function of chloride ion impermeability of concrete based on response surface model.

Based on the response surface model, the chloride ion migration coefficient of concrete is predicted, and the objective function of optimizing the chloride ion impermeability of concrete is established. The objective function for optimizing the chloride ion permeability of concrete is as follows:

$$\max \cdot f_2 = \max[RSM(x_1, x_2, \ldots, x_7)] = \beta'_0 + \sum_{i=1}^{7} \beta'_i x_i + \sum_{i=1}^{7} \beta'_{ii} x_i^2 + \sum_{i<j}^{7} \beta'_{ij} x_i x_j \tag{15}$$

(3) The objective function of concrete economic cost optimization

The costs of the raw materials employed in the concrete for the specific project under examination are presented in Table 5.

Table 5. Pricing information for the raw materials used in concrete.

Component	Units	Cost (Yuan)
Water	kg	0.0018
Cement	kg	0.4
Fly ash	kg	0.51
Fine aggregate	kg	0.12
Coarse aggregate	kg	0.14
Superplasticizer	kg	5.6
Polymer fiber	kg	7.8

Based on the above price information, the economic objective function of high-performance fiber-reinforced concrete is as follows:

$$\min \cdot f_3 = 0.0018x_1 + 0.4x_2 + 0.51x_3 + 0.12x_4 + 0.14x_5 + 5.6x_6 + 7.8x_7 \tag{16}$$

4.4.2. Using NSGA-III Algorithm for Durability and Economic Optimization

(1) Acquiring the Pareto optimal solution set for concrete mix proportions

In this investigation, the NSGA-III algorithm was characterized by a crossover rate of 0.7, a mutation rate of 0.01, a population size of 40, and a maximum generation limit of 80. Over the course of 80 iterations, the NSGA-III algorithm was applied to fulfill the durability specifications of high-performance fiber-reinforced concrete, concurrently aiming to achieve a noteworthy reduction in economic costs. Ultimately, the Pareto solution set for optimizing the mixture proportions of high-performance fiber-reinforced concrete was acquired, as depicted in Figure 6.

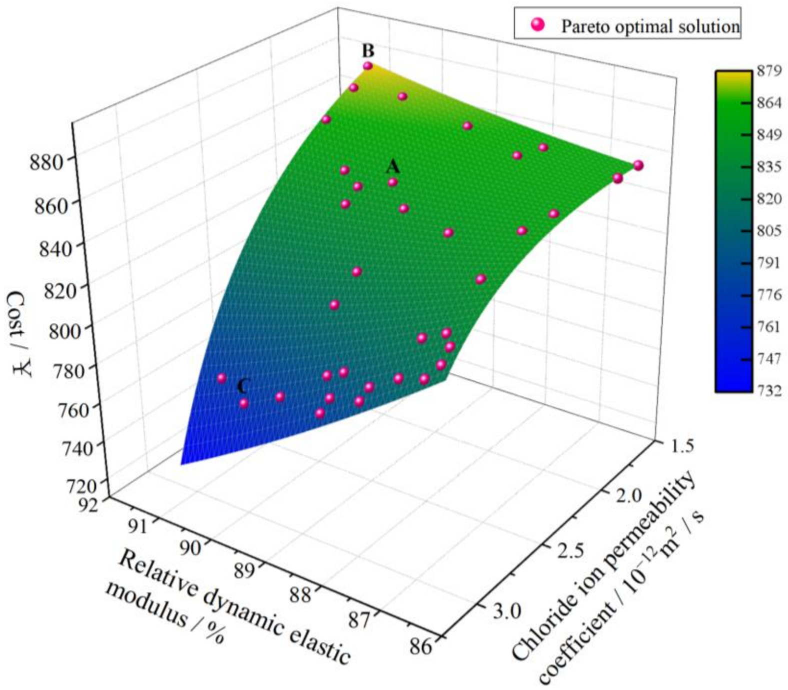

Figure 6. 3D View of the Pareto optimal solution.

Figure 6 illustrates the Pareto solution set obtained through the optimization of the mix ratio for high-performance fiber-reinforced concrete using the NSGA-III algorithm. On the horizontal axis of the figure, the relative dynamic elastic modulus and chloride ion permeability of high-performance concrete are depicted, serving as parameters to assess the durability of the concrete. Meanwhile, the vertical axis represents the cost associated with high-performance fiber-reinforced concrete.

By scrutinizing the variations in surface color, it becomes evident that, with an escalation in concrete cost, the surface color undergoes a discernible shift from deep blue to light green. The Pareto points concentrated in the blue region of the curved surface exhibit diminished values in both cost and durability indicators. As durability indicators advance, there is a concurrent increase in cost, signifying a positive correlation between the durability and cost of high-performance fiber-reinforced concrete. To a certain degree, augmenting the economic outlay of concrete can proficiently enhance its durability.

Figure 7 depicts the projections of Figure 6 on the freeze−thaw resistance and chloride permeability planes.

After applying optimization with NSGA-III, the frost resistance index of high-performance fiber-reinforced concrete lies within the 86% to 92% range. The optimized chloride ion migration coefficient varies within the range of 1.7 to 3.1 $\times$ 10^{-12} m^2/s, while the cost falls between 740 and 871 yuan. In accordance with the overarching trend observed in the Pareto optimization solution set, a trade-off is evident between the chloride ion permeability and the economic cost of high-performance fiber-reinforced concrete. Increasing the chloride ion migration coefficient leads to a proportional rise in economic expenses. In other words, enhancing the chloride ion resistance of concrete necessitates an increase in economic expenditure. In contrast, the relationship between the relative dynamic modulus of elasticity and economic costs for high-performance fiber-reinforced concrete remains inconclusive.

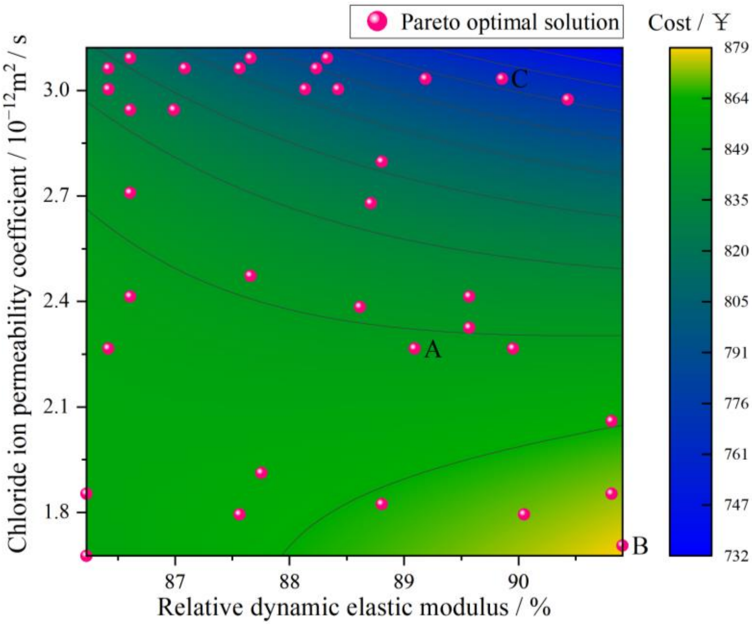

Figure 7. Projection of the Pareto optimal solution.

(2) The Selection and Analysis of the Pareto Solution Set for Optimizing Mix Proportion.

The Pareto solutions for optimizing each concrete mix proportion are derived through a meticulous consideration of the trade-offs inherent in multiple objectives. Put differently, there exists no singular solution capable of concurrently attaining both high concrete durability and low economic costs. Consequently, when confronted with diverse engineering projects, the imperative lies in selecting solutions that are aptly tailored to their specific requirements. In order to explicate this nuanced equilibrium, we designate Point A as the optimal balance obtained through the application of the ideal point method, comprehensively assessing the equilibrium between concrete durability and cost. Point B is delineated as the optimal solution, focusing predominantly on the performance of concrete durability, while Point C embodies the optimal solution, ensuring the minimization of economic costs in concrete. The intricate details of the specific parameters corresponding to Points A, B, and C along the Pareto boundary are meticulously elucidated in Table 6. These parameters serve as a scholarly guide for achieving optimal solutions amid diverse objective trade-offs, facilitating judicious decision-making in the realm of specific engineering projects.

Table 6. Pareto points on selected points and corresponding specific parameters.

Indicator	Item	Units	A	B	C
			Min	**Max**	**Ave**
Input indicator	x_1	kg/m^3	135	135	135
	x_2	kg/m^3	385	435	385
	x_3	kg/m^3	96	126	40
	x_4	kg/m^3	690	700	700
	x_5	kg/m^3	1129	1116	1116
	x_6	kg/m^3	4.96	4.16	4.16
	x_7	kg/m^3	48.72	48.3	42.1
	RD	%	89.20	90.91	87.24
	CP	10^{-12} m^2/s	2.18	1.76	2.91
	CO	yuan	851.85	878.78	766.56

(3) Validation of hybrid framework optimization effectiveness

To validate the efficacy of the hybrid algorithm optimization, we prepared concrete specimens in accordance with the aforementioned mixing ratio scheme and subsequently conducted durability tests on them. Table 7 presents a comparative analysis of predicted and experimental values for the concrete durability indicators.

Table 7. Analysis of predicted and experimental values of concrete durability indicators.

Optimization Plan for Mix Proportion	Anticipated Outcomes		Experimental Values		Errors	
	RD	CP	RD	CP	RD	CP
A	89.20	2.18	91.44	2.07	2.45%	5.31%
B	90.91	1.76	92.21	1.69	1.41%	4.14%
C	87.24	2.91	86.22	3.11	1.18%	6.43%

The disparity between the predicted values of RD and CP for concrete and their corresponding experimental values is minimal. In Scheme A, the errors for these two indicators are 2.45% and 5.31%, respectively. In Scheme B, the errors are 1.41% and 4.14%, respectively. Meanwhile, in Scheme C, the errors stand at 1.18% and 6.43% for these two indicators. The aforementioned outcomes substantiate the precision and dependability of the multi-objective optimization model founded on NSGA-III.

5. Discussion

The established multi-objective optimization model based on NSGA-III enables the optimization of three objectives, addressing the multi-objective conflicts encountered in practical engineering scenarios. To substantiate the heightened efficacy of the three-objective optimization relative to both single-objective and two-objective optimization, the optimization process was executed, considering frost resistance, chloride ion impermeability, and economic cost as objectives across varying quantities of objectives. The outcomes of the single-objective, two-objective, and three-objective optimization endeavors are delineated in Table 8.

Table 8. Optimization results of various quantitative indicators.

Optimization Objective		Anticipated Outcomes		
		CP	**RD**	**CO**
Single objective	CP	1.68	90.11	878.97
	RD	1.76	91.60	879.33
	CO	2.91	87.24	766.56
Two objectives	CD + RD	1.76	90.91	878.78
	CP + CO	1.72	89.95	871.36
	RD + CO	1.79	91.22	872.49
Three objectives	CP + RD + CO	2.18	89.20	851.85
Actual average		3.52	83.79	873.95

The results summarized in Table 8 indicate the following:

(1) In optimizing the mix proportion of high-performance fiber-reinforced concrete, the application of hybrid algorithms has yielded noteworthy outcomes. Whether pursuing single-objective optimization or multi-objective optimization, the achieved optimization values surpass the average experimental data, signifying the substantial advantages of this optimization method in enhancing concrete durability. Taking three-objective optimization as an illustration, the relative dynamic elastic modulus and chloride ion permeability coefficient are 89.20% and 2.18×10^{-12} m^2/s, respectively. In comparison, the corresponding average experimental values stand at 83.79% and 3.52×10^{-12} m^2/s. This marked improvement underscores the efficacy of multi-objective optimization. Consequently, this research offers robust theoretical underpinnings and practical insights for refining the mix proportion of high-performance fiber-reinforced concrete.

(2) Specificity of single-objective optimization: When using a genetic algorithm for single-objective optimization, the results were most tailored to the respective objective. The target values for chloride ion permeability, relative dynamic elastic modulus, and concrete economic cost obtained through single-objective genetic algorithm optimization were better than those from multi-objective genetic algorithm optimization, with optimized results of 1.68×10^{-12} m^2/s, 91.60%, and 766.56 yuan, respectively.

6. Conclusions

Currently, high-performance fiber-reinforced concrete (HPFRC) finds extensive applications in both domestic and international practical engineering projects. However, as the service environments for concrete structures become increasingly harsh, there is a growing demand for enhanced durability. Rational concrete mix design plays a crucial role in improving the durability of high-performance fiber-reinforced concrete, increasing the service life of concrete components, and reducing the overall life-cycle maintenance costs. Nevertheless, another essential objective in concrete mix design is cost reduction, which can sometimes conflict with the goal of improving durability. Traditional concrete mix design methods suffer from issues such as low efficiency and suboptimal results, making the multi-objective optimization of durability and economic costs for high-performance fiber-reinforced concrete a challenging task. Therefore, this article introduces an intelligent optimization framework based on hybrid algorithms. A Latin hypercube experimental design method is employed, considering factors such as water content, cement content, fly ash content, fine aggregate content, coarse aggregate content, superplasticizer dosage, and fiber dosage. Evaluation criteria include the relative dynamic modulus of elasticity, chloride ion resistance, and economic considerations. Response surface prediction models are established for each evaluation criterion. The NSGA-III algorithm is utilized within the RSM model to autonomously search for the optimal mix design that maximizes overall performance. Based on the optimization results and comparative experiments, the intelligent framework proposed in this article, leveraging hybrid algorithms, effectively optimizes the mix proportion of high-performance fiber-reinforced concrete. It not only meets durability requirements to a certain extent but also ensures cost control.

The hybrid algorithm proposed in this article can achieve multi-objective optimization of high-performance fiber-reinforced concrete within a certain range, but it also has certain limitations. The performance of machine learning models is usually influenced by the amount of training data, reliability, and complexity of the data. Even larger datasets may not necessarily improve the accuracy of the model. In machine learning, this can refer to "Kolmogorov complexity", which is the length of the shortest computer program that produces output. By reducing the complexity of the dataset, we can reduce the computational burden on the model when processing data, making it easier to capture patterns and correlations in the data. In this way, the model can predict and classify more accurately, thereby improving its accuracy. Therefore, when designing and preparing datasets, we should, to some extent, simplify the structure and features of the dataset to improve the performance of deep learning models.

The 36 sets of data used for training the model in this study were all from the same engineering project. Therefore, trained models may perform poorly in predicting specific data for other projects. In future research, collecting more diverse and specific data can better cover the characteristics and changes of different engineering projects and, to some extent, improve the generalization ability of the model. This means that the trained model can more accurately predict the specific data of other projects, rather than being limited to engineering projects with training data sources; it can reduce the bias and variance of the model and improve its reliability. This means that the model is more accurate and reliable in predicting and optimizing engineering materials. At the same time, constructing a hybrid algorithm that considers more parameters and objectives, further improving the effectiveness of multi-objective optimization, and promoting the development of new material design and optimization methods is our next research direction.

Author Contributions: Conceptualization, X.W. and F.C.; methodology, X.W. and F.C.; software, X.W.; validation, X.W., F.C. and D.J.; formal analysis, X.W.; investigation, F.C. and L.C.; resources, X.W.; data curation, F.C.; writing—original draft preparation, X.W.; writing—review and editing, L.C.; visualization, X.W.; supervision, D.J.; project administration, X.W. and F.C.; funding acquisition, X.W. All authors have read and agreed to the published version of the manuscript.

Funding: The research described in this paper was supported by the "Shandong Natural Science Foundation Project" (Project No. 60000101032). The authors greatly acknowledge their financial support.

Institutional Review Board Statement: Not applicable.

Informed Consent Statement: Not applicable.

Data Availability Statement: Data are contained within the article.

Conflicts of Interest: Long Cui was employed by the company Shandong Provincial Academy of Building Research Co., Ltd., Di Jiang was employed by the company Shandong Provincial Academy of Building Research Co., Ltd., the remaining authors declare that the research was conducted in the absence of any commercial or financial relationships that could be construed as a potential conflict of interest.

References

1. Habel, K.; Viviani, M.; Emmanuel, D.; Bruhwiler, E. Development of the mechanical properties of an Ultra-High Performance Fiber Reinforced Concrete (UHPFRC). *Cem. Concr. Res.* **2006**, *36*, 1362–1370. [CrossRef]
2. Habel, K.; Gauvreau, P. Response of ultra-high performance fiber reinforced concrete (UHPFRC) to impact and static loading. *Cem. Concr. Compos.* **2008**, *30*, 938–946. [CrossRef]
3. Abbas, S.; Soliman, A.M.; Nehdi, M.L. Exploring mechanical and durability properties of ultra-high performance concrete incorporating various steel fiber lengths and dosages. *Constr. Build. Mater.* **2015**, *75*, 429–441. [CrossRef]
4. Graybeal, B.A.; Hartmann, J.L. Strength and durability of ultra-high performance concrete. In Proceedings of the Concrete Bridge Conference, Taupo, New Zealand, 3–5 October 2003; p. 20.
5. Athanasopoulou, A.; Parra-Montesinos, G. Experimental Study on the Seismic Behavior of High-Performance Fiber-Reinforced Concrete Low-Rise Walls. *Aci Struct. J.* **2013**, *110*, 767–777.
6. Shehab, H.; Eisa, A.; Wahba, A.M.; Sabol, P.; Katunský, D. Strengthening of Reinforced Concrete Columns Using Ultra-High Performance Fiber-Reinforced Concrete Jacket. *Buildings* **2023**, *13*, 2036. [CrossRef]
7. Sheikh, S.A. Performance of concrete structures retrofitted with fiber reinforced polymers. *Eng. Struct.* **2002**, *24*, 869–879. [CrossRef]
8. Zhang, C.; Nerella, V.N.; Krishna, A.; Wang, S.; Zhang, Y.; Mechtcherine, V.; Banthia, N. Mix design concepts for 3D printable concrete: A review. *Cement Concr. Compos.* **2021**, *122*, 15. [CrossRef]
9. De Maeijer, P.K.; Craeye, B.; Snellings, R.; Kazemi-Kamyab, H.; Loots, M.; Janssens, K.; Nuyts, G. Effect of ultra-fine fly ash on concrete performance and durability. *Construct. Build. Mater.* **2020**, *263*, 13. [CrossRef]
10. Medvedev, V.; Pustovgar, A. A Review of Concrete Carbonation and Approaches to Its Research under Irradiation. *Buildings* **2023**, *13*, 1998. [CrossRef]
11. Niu, Z.; Lu, X.; Luo, Y. The Effects of a Multifunctional Rust Inhibitor on the Rust Resistance Mechanism of Carbon Steel and the Properties of Concrete. *Coatings* **2023**, *13*, 1375. [CrossRef]
12. Li, W.; Hu, S. Fracture Behavior of Concrete under Chlorine Salt Attack Exposed to Freeze–Thaw Cycles Environment. *Materials* **2023**, *16*, 6205. [CrossRef] [PubMed]
13. Dai, J.; Wang, Q.; Zhang, B. Frost resistance and life prediction of equal strength concrete under negative temperature curing. *Constr. Build. Mater.* **2023**, *396*, 132278. [CrossRef]
14. Wang, Y.; Liu, Z.; Fu, K.; Li, Q.; Wang, Y. Experimental studies on the chloride ion permeability of concrete considering the effect of freeze–thaw damage. *Constr. Build. Mater.* **2020**, *236*, 117556. [CrossRef]
15. Liu, D.; Tu, Y.; Shi, P.; Sas, G.; Elfgren, L. Mechanical and durability properties of concrete subjected to early-age freeze–thaw cycles. *Mater. Struct.* **2021**, *54*, 211. [CrossRef]
16. Nosouhian, F.; Mostofinejad, D.; Hasheminejad, H. Influence of biodeposition treatment on concrete durability in a sulphate environment. *Biosyst. Eng.* **2015**, *133*, 141–152. [CrossRef]
17. Wu, Y.; Ren, Q.; Zhang, X. Compressive behavior and freeze-thaw durability of concrete after exposure to high temperature. *Eur. J. Environ. Civ. Eng.* **2022**, *26*, 6830–6844. [CrossRef]
18. Kou, S.C.; Poon, C.S.; Chan, D. Influence of fly ash as cement replacement on the properties of recycled aggregate concrete. *J. Mater. Civ. Eng.* **2007**, *19*, 709–717. [CrossRef]
19. Mehta, P.K. Influence of fly ash characteristics on the strength of portland-fly ash mixtures. *Cem. Concr. Res.* **1985**, *15*, 669–674. [CrossRef]
20. Atiş, C.D.; Karahan, O. Properties of steel fiber reinforced fly ash concrete. *Constr. Build. Mater.* **2009**, *23*, 392–399. [CrossRef]

21. Karahan, O.; Atiş, C.D. The durability properties of polypropylene fiber reinforced fly ash concrete. *Mater. Des.* **2011**, *32*, 1044–1049. [CrossRef]
22. *JGJ 55—2011*; Specification for Mix Proportion Design of Ordinary Concrete. Ministry of Housing and Urban-Rural Construction of the People's Republic of China: Beijing, China, 2011.
23. Chopra, P.; Kumar, R.; Kumar, M. Artificial Neural Networks for the Prediction of Compressive Strength of Concrete. *Int. J. Appl. Sci. Eng.* **2015**, *13*, 187–204.
24. Alsanusi, S.; Bentaher, L. Prediction of Compressive Strength of Concrete from Early Age Test Result Using Design of Experiments (RSM). *Int. J. Civ. Environ. Struct. Constr. Archit. Eng.* **2015**, *9*, 1522–1526.
25. Qurishee, M.A.; Iqbal, I.T.; Islam, M.S.; Islam, M.M. Use of Slag As Coarse Aggregate and Its Effect on Mechanical Properties of Concrete. In Proceedings of the 3rd International Conference on Advances in Civil Engineering, CUET, Chittagong, Bangladesh, 21–23 December 2016.
26. Xu, Y.; Li, M.; Zhao, X.; Lu, F. The response curved surface regression analysis technique the application of a new regression analysis technique in materials research. *Rare Met. Mater. Eng.* **2001**, *30*, 428–432.
27. Li, L.; Zhang, S.; He, Q.; Hu, X.B. Application of response surface methodology in experiment design and optimization. *Res. Explor. Lab.* **2015**, *34*, 41–45.
28. Zhang, L.; Sojobi, A.; Kodur, V.; Liew, K. Effective utilization and recycling of mixed recycled aggregates for a greener environment. *J. Clean. Prod.* **2019**, *236*, 117600. [CrossRef]
29. Alyamac, K.E.; Ghafari, E.; Ince, R. Development of eco-efficient self-compacting concrete with waste marble powder using the response surface method. *J. Clean. Prod.* **2017**, *144*, 192–202. [CrossRef]
30. Tyagi, M.; Rana, A.; Kumari, S.; Jagadevan, S. Adsorptive removal of cyanide from coke oven wastewater onto zero-valent iron:Optimization through response surface methodology, isotherm and kinetic studies. *J. Clean. Prod.* **2018**, *178*, 398–407. [CrossRef]
31. Sim¸sek, B.; Uygunoğlu, T.; Korucu, H.; Kocakerim, M.M. Analysis of the effects of dioctyl terephthalate obtained from polyethylene terephthalate wastes on concrete mortar: A response surface methodology based desirability function approach application. *J. Clean. Prod.* **2018**, *170*, 437–445. [CrossRef]
32. Taherkhani, H.; Noorian, F. Investigating permanent deformation of recycled asphalt concrete containing waste oils as rejuvenator using response surface methodology (RSM). *Iran. J. Sci. Technol. Trans. Civ. Eng.* **2021**, *45*, 1989–2001. [CrossRef]
33. Bheel, N.; Mohammed, B.S.; Liew, M.S.; Zawawi, N.A.W.A. Effect of Graphene Oxide as a Nanomaterial on the Durability Behaviors of Engineered Cementitious Composites by Applying RSM Modelling and Optimization. *Buildings* **2023**, *13*, 2026. [CrossRef]
34. Wang, J.; Wang, W. Response surface based multi−objective optimization of basalt fiber reinforced foamed concrete. *Mater. Rep.* **2019**, *33*, 4092–4097.
35. Zhang, Q.; Feng, X.; Chen, X.; Lu, K. Mix design for recycled aggregate pervious concrete based on response surface methodology. *Constr. Build. Mater.* **2020**, *259*, 119776. [CrossRef]
36. DeRousseau, M.A.; Kasprzyk, J.R.; Srubar, W.V. Multi-objective optimization methods for designing low-carbon concrete mixtures. *Front. Mater.* **2021**, *8*, 13. [CrossRef]
37. Nguyen, T.T.; Thai, H.T.; Ngo, T. Optimised mix design and elastic modulus prediction of ultra-high strength concrete. *Construct. Build. Mater.* **2021**, *302*, 124150. [CrossRef]
38. Sun, H.; Burton, H.V.; Huang, H.L. Machine learning applications for building structural design and performance assessment: State-of-the-art review. *J. Build. Eng.* **2021**, *33*, 14. [CrossRef]
39. Zavala, G.R.; Nebro, A.J.; Luna, F.; Coello Coello, C.A. A survey of multi-objective metaheuristics applied to structural optimization. *Struct. Multidiscip. Optim.* **2014**, *49*, 537–558. [CrossRef]
40. Srinivas, N.; Deb, K. Multiobjective function optimization using nondominated sorting genetic algorithms. *Evol. Comput.* **1995**, *2*, 221–248. [CrossRef]
41. Deb, K.; Pratap, A.; Agarwal, S.; Meyarivan, T. A fast and elitist multiobjective genetic algorithm: NSGA-II. *IEEE Trans. Evol. Comput.* **2002**, *6*, 182–197. [CrossRef]
42. Bolon-Canedo, V.; Remeseiro, B. Feature selection in image analysis: A survey. *Artif. Intell. Rev.* **2020**, *53*, 2905–2931. [CrossRef]
43. Kabir, H.; Garg, N. Machine learning enabled orthogonal camera goniometry for accurate and robust contact angle measurements. *Sci. Rep.* **2023**, *13*, 1497. [CrossRef]
44. Deb, K.; Jain, H. An Evolutionary Many-objective optimization algorithm using reference-point based non-dominated sorting approach part I: Solving problems with box constraints. *IEEE Trans. Evol. Comput.* **2014**, *18*, 577–601. [CrossRef]
45. Zhang, J.; Wang, S.; Tang, Q.; Zhou, Y.; Zeng, T. An improved NSGA-III integrating adaptive elimination strategy to solution of many-objective optimal power flow problems. *Energy* **2019**, *172*, 945–957. [CrossRef]
46. Ruan, F.; Gu, R.; Huang, T.; Xue, S. A big data placement method using NSGA-III in meteorological cloud platform. *EURASIP J. Wirel. Commun. Netw.* **2019**, *2019*, 143. [CrossRef]
47. Yuan, X.; Tian, H.; Yuan, Y.; Huang, Y.; Ikram, R.M. An extended NSGA-III for solution multi-objective hydro-thermal-wind scheduling considering wind power cost. *Energy Convers. Manag.* **2015**, *96*, 568–578. [CrossRef]
48. Liu, Y.; You, K.; Jiang, Y.; Wu, Z.; Liu, Z.; Peng, G.; Zhou, C. Multi-objective optimal scheduling of automated construction equipment using non-dominated sorting genetic algorithm (NSGA-III). *Autom. Constr.* **2022**, *143*, 104587. [CrossRef]

49. Jafari, H.; Nazif, S.; Rajaee, T. A multi-objective optimization method based on NSGA-III for water quality sensor placement with the aim of reducing potential contamination of important nodes. *Water Supply* **2022**, *22*, 928–944. [CrossRef]
50. Zaifang, Z.; Feng, X.; Xiwu, S. Multi-objective Optimization of Hydroforming Process of Rocket Tank Bottom. *J. Mech. Eng.* **2022**, *58*, 78–86.
51. Kumar, U.; Klefsjö, B. Reliability analysis of hydraulic systems of LHD machines using the power law process model. *Reliab. Eng. Syst. Saf.* **1992**, *35*, 217–224. [CrossRef]
52. Sriravindrarajah, R.; Wang, N.D.H.; Ervin, L.J.W. Mix design for pervious recycled aggregate concrete. *Int. J. Concr. Struct. Mater.* **2012**, *6*, 239–246. [CrossRef]
53. Stein, M. Large Sample Properties of Simulations Using Latin Hypercube Sampling. *Technometrics* **1987**, *29*, 143–151. [CrossRef]
54. Owen, A.B. A Central Limit Theory for Latin Hypercube Sampling. *J. R. Stat. Soc. Ser. B* **1992**, *54*, 541–551.
55. Olsson, A.; Sandberg, G.; Dahlblom, O. On Latin hypercube sampling for structural reliability analysis. *Struct. Saf.* **2003**, *25*, 47–68. [CrossRef]
56. *GBT 50476-2019*; Durability Design Standard for Concrete Structures. Ministry of Housing and Urban-Rural Development of the People's Republic of China: Beijing, China, 2019.